American Journal of Biochemistry and Biotechnology

Original Research Paper

Optimization of Ultrasonic-Assisted Total Flavonoids Extraction from Flower of *Albizia Julibrissin* Durazz. by Response Surface Methodology for Characterization of Chemical Profile and Evaluation of Antioxidant and Tyrosinase Inhibitory Activities

[2]Yijie Cheng, [1]Yuwen Zhang, [1]Hanzhang Sun, [1]Dongting Huang, [1]Bo Jiang, and [1]Jingyuan Xu

[1]School of Biology and Food Engineering, Changshu Institute of Technology, Changshu, China
[2]First People's Hospital of Changshu City, Changshu Hospital Affiliated to Soochow University, Changshu, China

Article history
Received: 14-01-2022
Revised: 14-02-2022
Accepted: 16-02-2022

Corresponding Author:
Jingyuan Xu
School of Biology and Food Engineering, Changshu Institute of Technology, Changshu, China
Email: jingyuanxu369@gmail.com

Abstract: To investigate the flavonoids in the flower of *Albizia julibrissin* ('He Huan Hua' in Chinese), the ultrasonic-assisted extraction of total flavonoids from 'He Huan Hua' was optimized by response surface methodology and the chemical profile was characterized by HPLC-QTOF-MS/MS. What's more, the antioxidant and tyrosinase inhibitory activities of 'He Huan Hua' were also evaluated in this study. The extraction time, extraction temperature, and ethanol concentration were optimized by single-factor experiments and response surface methodology. The three factors were optimized to be 43 min, 40°C, and 49% (v/v) respectively. Under the optimized extraction condition, the yield of total flavonoids from 'He Huan Hua' was 3.31% (W/W). There were 32 different flavonoids identified from the extracts of 'He Huan Hua', which mainly were flavonol glycosides and the principal component was quercitrin. The antioxidant activity of the extracts of 'He Huan Hua' was evaluated by Diphenyl Picryl Hydrazinyl Radical (DPPH), 2,2′-Azinobis (3-ethylbenzothiazoline-6-sulfonic acid) (ABTS), and reducing power assays. The extracts of 'He Huan Hua' exhibited good antioxidative activity with IC_{50}/EC_{50} of 90.91±3.36 (DPPH assay), 15.09±0.17 (ABTS assay), and 67.69±2.97 (reducing power assay) μg/mL, respectively. Most importantly, the extracts of 'He Huan Hua' also showed good tyrosinase inhibitory activity (IC_{50}:1.32±0.01 mg/mL). The higher antioxidant and tyrosinase inhibitory activities of 'He Huan Hua' might be related to the presence of rich flavonol compounds. In summary, flavonoids in 'He Huan Hua' have great value for developing antioxidants and tyrosinase inhibitors and are deserved to be applied for the prevention of premature skin aging.

Keywords: *Albizia Julibrissin* Durazz, Chemical Profile, Antioxidant Activity, Tyrosinase Inhibitory Activity, Response Surface Methodology

Introduction

Excessive production of Reactive Oxygen Species (ROS) in skin cells can induce oxidative stress and has been verified as a major cause of premature skin aging (Cruciani *et al*., 2021; Lee *et al*., 2021). Elimination of excessive ROS by exogenous supplement of antioxidants can prevent skin from oxidative stress-induced damage (Lavigne *et al*., 2022). Hyperpigmentation also can result in different dermatological disorders such as premature skin aging (Hałdys *et al*., 2018). It is well known that tyrosinase is the key enzyme for melanin synthesis in the skin and inhibiting tyrosinase activity can relieve pigmentation

(Bourhim *et al*., 2021; Arroo *et al*., 2020). Thus, the development of effective antioxidants and tyrosinase inhibitors is of great significance for the prevention of premature skin aging.

The flower of *Albizia Julibrissin* Durazz., 'He Huan Hua' in Chinese, is widely consumed as scented tea and Chinese medicine in China (CPC, 2020). Previous studies have shown that 'He Huan Hua' is rich in flavonoids (Kang *et al*., 2000; Yahagi *et al*., 2012). Substantial pieces of evidence have suggested that flavonoids in herbal medicine always exhibit good antioxidant and tyrosinase inhibitory activities (Li *et al*., 2021). It can be speculated that the flavonoids in 'He Huan Hua' may have potential value for developing antioxidants and tyrosinase inhibitors. However, the chemical profile and related bioactivities of 'He Huan Hua' have not been fully investigated so far. It has limited the further application of 'He Huan Hua' for solving skin health issues.

To characterize the chemical profile or assess the bioactivities of natural products in plants, the extraction method should be optimized first to make sure that the target compositions are adequately extracted. Compared with other conventional extraction methods, the ultrasonic-assisted extraction method has obvious advantages such as shorter extraction time, lower extraction temperature, and higher yield rate (Yuan *et al*., 2015). Due to the above characteristics, the ultrasonic-assisted extraction method has been used for flavonoid extraction from medicinal plants (Zuo *et al*., 2022). At present, few studies have investigated the ultrasonic-assisted total flavonoids extraction method from 'He Huan Hua' and the influences of extraction factors on the extraction method have not been clarified. Response Surface Methodology (RSM) is a powerful statistical technique. Since it can predict the optimum experimental factors by the mathematical model with few tests, RSM has been widely used to optimize extraction schemes and provide information on independent variables on one or more responses (Cui *et al*., 2018).

Therefore, in this research, the total flavonoids in 'He Huan Hua' were extracted by ultrasonic-assisted extraction method, and extraction factors were optimized by RSM. The chemical profile of the Extracts of Flower of *A. julibrissin* (EFA) was characterized by HPLC-QTOF-MS/MS and its antioxidant and tyrosinase inhibitory activities were assessed *in vitro*. The flow chart of the research methodology was showed in Fig. 1. This study will provide a basis for screening antioxidants and tyrosinase inhibitors from 'He Huan Hua' and discover the application value of 'He Huan Hua' for the prevention of premature skin aging.

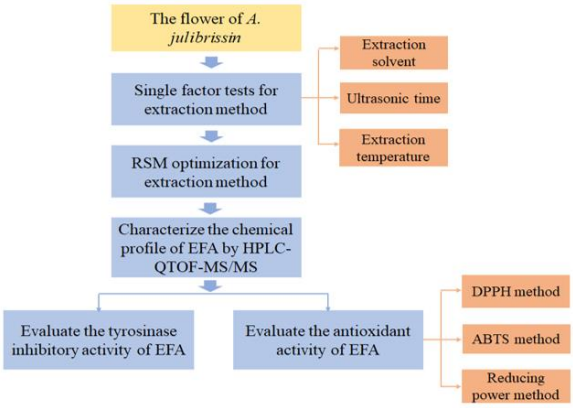

Fig. 1: Flow chart of research methodology in this study

Materials and Methods

Plant Materials

'He Huan Hua' was collected from the campus of Changshu Institute of Technology (Changshu, China) and identified by Professor Minjian Qin. The herbarium samples (Voucher No.AJD-01) were deposited at the School of Biotechnology and Food Engineering, Changshu Institute of Technology, Changshu, China. The samples were placed in a cool and ventilated room for natural drying. The dry samples were ground to 50 meshes and stored at room temperature before extraction.

Chemicals and Reagents

Quercitrin, quercetin, and rutin purchased from Baoji Herbest Biotechnology (Baoji, China) were used as reference standards. The purities of the reference standards were over 98% determined by HPLC analysis. The methanol used for high-resolution mass spectrometry was purchased from Merck (Darmstadt, Germany). Preparation of deionized water was through Merck Millipore Direct-Q3 (Marlborough, MA, U.S.A). DPPH and ABTS were purchased from Sangon Biotech Co. Ltd. (Shanghai, China). Tyrosinase (from mushroom) was purchased from Sigma-Aldrich (St Louis, MA, U.S.A.). The other analytical grade reagents were purchased from Nanjing Chemical Regents Co. Ltd. (Nanjing, China).

Ultrasonic-Assisted Extraction Method

Firstly, the extraction conditions (extraction solvent, extraction time, and extraction temperature) were optimized through single-factor experiments. The accurately weighed dry sample powder (0.3 g) was ultrasonicated in ethanol aqueous (25 mL) for a while and cooled to room temperature. After that, the extraction solution was centrifuged at 4,000 g for 10 min and the supernatant was transferred. Repeat this step once. The supernatant was mixed and adjusted to 50 mL with ethanol solution. Then, the extraction solution of 'He Huan Hua' was stored at 4°C until use.

Determination of the Extraction Yield of Total Flavonoids

The concentrations of total flavonoids in the extraction solution of 'He Huan Hua' was determined according to the published literature with modification (Sarikurkcu *et al*., 2015). 1 mL of extraction solution and 8 mL of aluminum chloride solution (dissolved in methanol, 1%, w/v) were mixed. After that, the volume of the mixture was adjusted to 25 mL with ethanol solution (48%, V/V). After reacting for 15 min at room temperature, the mixture was measured at 272 nm by ultraviolet spectrophotometry. Different concentration solutions of quercetin were used as a standard substance for calibration.

The concentration of total flavonoids in the sample solution was calculated by calibration curve (Eq. 1) and the extraction yield of total flavonoids was calculated by Eq. (2).

The calibration curve for determination of total flavonoids concentration:

$$A = 2.5429C - 0.0132, R^2 = 0.9999 \quad (1)$$

where:

A = The absorbance
C = The concentration of total flavonoids in extraction solution (mg/mL)

The extraction yield of total flavonoids (%) was calculated as follows:

$$R(W/W,\%) = \frac{C \times 50mL}{Ws} \times 100\% \quad (2)$$

where:

C = The concentration of total flavonoids in the sample solution (mg/mL)
W_s = The weight of the sample (mg)
R (w/w, %) = The extraction yield of total flavonoids

RSM Experimental Design and Statistical Analysis

The RSM was used to optimize the extraction conditions by analyzing the relationship between variables and response. Box-Behnken (BBD) is one of the most common RSM experimental designs that had been widely used to optimize extraction conditions (Ahmad *et al*., 2015). Therefore, the extraction process of total flavonoids was optimized by a three-factor three-level BBD. The regression analysis of experimental results was performed by Design-Expert software (version 8.0.6, Stat-Ease Inc., Minneapolis, Minnesota). The three independent variables were extraction temperature (X_1), extraction time (X_2), and ethanol concentration (X_3). The ranges and center point values of the three variables were shown in Table 1. The model was developed by the following equation:

$$Y = A_0 + \sum_{i=1}^{n} A_i X_i + \sum_{i=1}^{n} A_{ii} X_i^2 + A_{ij} X_i X_j \quad (3)$$

where:

Y = The predicted extraction rate of total flavonoids
A_0 = The constant-coefficient
A_i, A_{ii}, and A_{ij} = The linear, quadratic, and interaction coefficients, respectively
X_i and X_j = The levels of independent variables

Chemical Composition Qualitative Analysis by UPLC-QTOF-MS/MS

Waters ACQUITY UPLC (Waters, Massachusetts, USA) was used for chromatographic separation. An ACQUITY UPLC BEH-C18 column (3.0 × 50 mm, 1.7 μm, Waters, Ireland) was used for analysis at 30°C. The mixture of 0.1% formic acid-water (A) and methanol (B) was used as the mobile phase for chromatographic separation. The flow rate was 0.3 mL/min and the gradient conditions were: 0-5 min, 20-30% (B), 5-15 min, 30-55% (B), 15-20 min, 55-95%, 20-21 min, 95-20%, 21-25 min, 20%. The injection volume was 5 μL.

The qualitative analysis of EFA was performed by the AB SCIEX Triple TOF^{TM} 5600^{+} system (AB SCIEX Technologies, Redwood City, CA, USA) in negative ion mode. The mass system was equipped with an electrospray ion source. The mass range was set from 100 to 2000 m/z. The electrospray ionization temperature was 50°C. The nebulizer gas pressure, ion spray voltage, and collision energy were 60 psi, 4.5 VK, and -50 V respectively.

Antioxidant Activity

DPPH Scavenging Assay

To assess the antioxidant activity of EFA, a DPPH scavenging assay was used with slight modifications (Khochapong *et al*., 2021). Firstly, EFA was prepared at different concentrations. After that, 0.5 mL of EFA solution was mixed with 6 mL of 0.1 mmol/L DPPH solution. The mixed solution was left to react for 30 min at room temperature, protected from light. Subsequently, the absorbance of the mixed solution was measured at 517 nm. Ascorbic acid (V_C) was used as a positive control. The DPPH radical scavenging activity was calculated as follows:

$$scavenging\ activity(\%) = \frac{A_0 - (A_1 - A_2)}{A_0} \times 100\% \quad (4)$$

where:

A_0 = The absorbance of control
A_1 = The absorbance of the EFA (or V_C) group
A_2 = The absorbance of blank without DPPH

ABTS Scavenging Activity

The reported ABTS scavenging assay was used to evaluate the antioxidant activity of EFA (Ha *et al*., 2021). The ABTS stock solution was prepared by mixing the same volume of ABTS solution and potassium persulfate solution. Before being used, the ABTS stock solution should be stored at room temperature for 16 h and then diluted until its absorbance at 734 nm close to 0.7. After that, the EFA solution and the diluted ABTS solution were mixed and incubated in dark at 30°C for 30 min. The absorbance of the mixture was measured at 734 nm. The ABTS radical scavenging activity was calculated as follows:

$$scavenging\ activity(\%) = \frac{A_0 - (A_1 - A_2)}{A_0} \times 100\% \quad (5)$$

where, A_0, A_1, and A_2 were the control, the absorbance values of the EFA (or V_C) group, and the blank without ABTS, respectively.

Reducing Power Assay

The antioxidant activity of EFA was also evaluated by reducing power assay (Xie *et al*., 2021). Firstly, the EFA solution was mixed with 1.5 mL phosphate buffer (0.2 mol/L, pH6.6) and 1.5 mL potassium ferricyanide (1%, W/V) solution. Then, the mixture solution was incubated at 50°C for 20 min. After incubation, 1.5 mL of trichloroacetic acid (10%, w/v) was added to the mixture and centrifuged. The supernatant of the mixture was recovered and mixed with 0.6 mL of anhydrous Iron (III) chloride ($FeCl_3$) (1 mg/mL) and 3 mL of distilled water. After incubated at room temperature for 30 min, the absorbance of the mixture was measured at 700 nm and its EC_{50} value was calculated. Vc was used as a positive control.

Tyrosinase Inhibitory Activity

The tyrosinase inhibitory activity of EFA was evaluated by the published method with a slight modification (Yang *et al*., 2019). Before determination, the evaporated EFA was dissolved in phosphate buffer (0.2 mol/L, pH6.8, PBS) and diluted to different concentrations. Then, 70 μL of EFA solution, 200 μL of tyrosinase solution (dissolved in PBS, 200 U/mL), and 360 μL PBS were mixed and incubated at 37°C for 10 min. After that, 70 μL of L-DOPA (5 mmol/L, dissolved in PBS) was added to the mixture. After reacting for 20 min, the absorbance of the mixed solution was measured at 475 nm by using a Microplate Reader (Epoch, Biotek, USA).

Table 1: Experimental values of response variables for BBD

Run	Independent variables			Dependent variables
	X_1[a]	X_2[b]	X_3[c]	Y[d]
1	0	-1	1	1.51
2	-1	0	-1	2.47
3	-1	0	1	1.16
4	-1	-1	0	2.68
5	1	-1	0	2.86
6	0	0	0	3.27
7	0	0	0	3.34
8	1	1	0	3.09
9	0	-1	-1	2.76
10	-1	1	0	2.96
11	0	1	1	1.77
12	1	0	-1	2.56
13	0	0	0	3.23
14	0	0	0	3.19
15	0	0	0	3.33
16	0	1	-1	2.96
17	1	0	1	1.96

[a]X_1, extraction temperature (°C), three different levels (-1, 0, 1) represented 16, 37 and 58
[b]X_2, extraction time (min), three different levels (-1, 0, 1) represented 10, 30 and 50
[c]X_3, ethanol concentration (%), three levels (-1, 0, 1) represented 20, 60 and 100
[d]Y, extraction rate of total flavonoids from 'He Huan Hua' (%)

V_C was used as a positive control. Tyrosinase inhibition activity was calculated as follows:

$$Inhibition\,activity\,(\%) = \frac{(A_c - A_d) - (A_a - A_b)}{A_c - A_d} \times 100\% \quad (6)$$

where,

A_a = The absorbance of the reaction system including EFA or Vc, tyrosinase, and L-DOPA
A_b = The absorbance of the reaction system without tyrosinase
A_c = The absorbance of the reaction system without EFA (or Vc)
A_d = The absorbance of the reaction system only containing L-DOPA

Statistical Analysis

In this study, each experiment was performed in triplicate. The data were illustrated as mean ± standard deviation. Statistical analysis was performed using SPSS (v. 14.0; SPSS Inc., Chicago, IL, USA). Values were considered significant when the p-value was lower than 0.05.

Results

Single-Factor Experiments for Optimizing Ultrasounds Assisted Extraction Condition

The extraction rate of flavonoids from crude plant materials was affected by many factors. It has been reported that the extraction solvent, ultrasonic time, and ultrasonic temperature were key factors to improve the extraction rate by ultrasound-assisted extraction method (Yu *et al*., 2021). Therefore, in this study, the influence of these factors on the yield rate of total flavonoids was firstly evaluated by single-factor experiments.

When extraction solvent has similar polarity with target components, natural products will dissolve in extraction solvent more sufficiently. As the polarity of ethanol aqueous changes with the concentration of ethanol, the appropriate concentration of ethanol must be investigated. In this part, the extraction rate of the total flavonoids was compared under different concentrations of ethanol. As shown in Fig. 2A, the extraction rate of total flavonoids changed with different concentrations of ethanol. The extraction rate of total flavonoids increased significantly when the concentration of ethanol solution increased from 20 to 40%. After that, the extraction rate remained stable even though the concentration of ethanol increased continuously. When the concentration of ethanol reached 100%, the yield rate of the total flavonoids decreased. Yuan *et al*. (2012) also found a similar change rule of the extraction yield of total flavonoids in the Huan Hua when extracted with different concentration ethanol solutions. For environmental protection and saving solvent, the optimum concentration of ethanol was set at 40%.

The extraction time was the second factor investigated. The extraction time was set from 10 to 50 min. When extraction time changed, the concentration of ethanol was kept at 40% and the extraction temperature was kept at 25℃, consistently. The results indicated that the extraction rate of total flavonoids elevated gradually within 30 min and reached the maximum when extracted for 30 min (Fig. 2B). After that, the extraction rate of total flavonoids decreased. Therefore, 30 min was the appropriate time for sufficient extraction of total flavonoids.

In addition to extraction solvent and extraction time, extraction temperature could also influence the yield rate of total flavonoids when using the ultrasound-assisted extraction method. In this research, the extraction temperature was set from 15 to 60℃ with the concentration of ethanol at 40% and an extraction time of 30min. The extraction rate of the total flavonoids increased significantly when the extraction temperature rose from 15 to 30℃ and kept consistently when the extraction temperature changed from 30 to 45℃. However, with the extraction temperature rising continuously, the extraction rate of the total flavonoids decreased (Fig. 2C). The partial reason for this phenomenon might be due to the high temperature-induced decrease of dissolved gas in the extraction solution, which led to the weakening of cavitation and the decrease in extraction rate (Song *et al*., 2014). Except that, more non-flavonoid compounds in ‘He Huan Hua’ would be extracted at a higher extraction temperature (Yuan *et al*., 2013). Thus, the best extraction temperature was set at 30℃.

Optimization of Ultrasounds Assisted Extraction Method by RSM

As the optimal extraction condition was the result of the interaction of multiple factors, the three factors were optimized by RSM subsequently based on the results of single-factor tests. The BBD matrix consisted of 17 experiments and three factors (ethanol concentration, extraction time, and extraction temperature). The results of all 17 experiments were presented in Table 1. Based on the experimental data,

a quadratic regression analysis was performed. The predicted regression equation was as follows:

$$Y = 3.27 + 0.15X_1 + 0.12X_2 - 0.54X_3 - 0.012X_1X_2 + 0.18X_1X_3 + 0.016X_2X_3 - 0.29X_1^2 - 0.083X_2^2 - 0.94X_3^2 \quad (7)$$

Where:
Y = The extraction rate of the total flavonoids
X_1 = The values of extraction temperature
X_2 = The values of extraction time
X_3 = The values of ethanol concentration

The RSM model coefficients were validated by ANOVA. As shown in Table 2, the F-value of the model was 59.72 and the P-value of the model was less than 0.0001. It indicated that the model was statistically significant (Sunday, 2020). The lack-of-fit analysis was always applied to judge the difference between the obtained model and the actual situation. In this study, the *P*-value of the lack-of-fit was larger than 0.05. It indicated that the extraction rate predicted by the regression equation had no significant difference from the actual experimental results. In addition, the coefficient of determination (R_2) and adjusted coefficient of determination (Adj.R_2) were 0.9871 and 0.9706, which showed that the difference between obtained mode and the actual situation was less than 3%. All the above results indicated that the regression model (Eq. 7) was appropriate to predict the optimal condition of the ultrasonic-assisted extraction method.

Through the RSM, the contour plots and the three-dimensional response curves were obtained to visualize the interaction effect of two independent extraction factors on extraction rate. The shape and curvature of the response surface plot can reflect the influence of the interaction between different factors on response value to some extent (Sady *et al*., 2019). The shape of the response surface can reflect the changing pattern of response value when interaction factors change and the curvature of the response surface could reflect the degree of influence of the interaction factor on response value. The greater curvature of the response surface meant a more obvious influence of the interaction of related factors on response values (Xie *et al*., 2017). As shown in Fig. 3, the similar shape of response surface plots meant a similar change pattern in the yield rate of total flavonoids in three different interactions. In addition, the response surface plot in Fig. 3B showed a steeper profile than the other two plots. It meant that the interaction between ethanol concentration (X_3) and extraction temperature (X_1) had the most significant effect on the extraction rate of total flavonoids when using the ultrasound-assisted extraction method. It was consistent with the results of ANOVA in Table 2.

According to the established response surface model, the optimal condition of ultrasound-assisted total flavonoid extraction was predicted as follows: Extraction temperature of 40.32°C, extraction time of 43.85 min, and ethanol concentration of 49.30%. Under this condition, the predicted yield rate of the total flavonoids was 3.40%. To evaluate the accuracy of the predicted optimal extraction condition, the total flavonoids were extracted based on the predicted extraction condition with slight modification. The extraction condition was as follows: Extraction temperature of 40°C, extraction time of 43 min, and ethanol concentration of 49%. The actual yield rate of the total flavonoids was 3.31% with a deviation from the predicted value of less than 3%. Therefore, the established response surface model could be effectively used to optimize the ultrasonic-assisted extraction condition.

The Chemical Profile of EFA

'He Huan Hua' was rich in flavonoids, but the chemical profile of 'He Huan Hua' was still unclearly. In this study, we developed a simple, rapid, and sensitive UPLC-QTOF-MS/MS method to characterize the chemical profile of 'He Huan Hua' within 25 min (Fig. 4A). A total of 32 compounds were identified in EFA and eight of these compounds were reported in 'He Huan Hua' for the first time (as shown in Table 3). These identified compounds have almost belonged to flavonol glycosides.

The compounds were identified in the following process. Firstly, the detected accurate mass values of deprotonated molecular ions and the empirical molecular formula were matched with the reported data. Subsequently, the confirmation was further performed by comparing fragmentation ions. Under the negative mode, the identified compound showed $[M-H]^-$ ions and flavonol glycosides were deduced by successive losses of glycosyls, such as hexose (m/z 162 or m/z 146), pentose (m/z 132), or rutinose (m/z 308), while the information of additional fragment ions was used as supplementary for further identification. The compound 16 was characterized as a typical flavonol glycoside, which showed a deprotonated molecular ion at m/z 447.0955 with the molecular formula $C_{21}H_{19}O_{11}^-$. The fragment ion at

m/z 301.0379 showed the deprotonated molecular ion lost a rhamnose residue [M-H-146]$^-$ and the fragment ion at m/z 300.0301 showed the deprotonated molecular ion lost a rhamnose residue and a hydrion [M-H-147]$^-$. Further dissociation of the aglycone ion m/z 300.0301 [M-H-$C_6H_{11}O_4$]$^-$ might yield a series of fragments. The fragment ions at m/z 271.0272 and 255.0321 might come from the aglycone ion m/z 300.0301 with losses of neutral fragments CHO and [CO+OH] respectively. The fragment ions at m/z 271.0272 might further be lost neutral fragments CO and generated the fragment ions 243.0317 [M-H-$C_6H_{11}O_4$-CHO-CO]$^-$ and 227.0363 [M-H-$C_6H_{11}O_4$-CHO_2-CO]$^-$. The extracted ion chromatogram and the fragmentation pattern were shown in Fig. 4B and 4C. In comparison with the reference standard (Fig. 5A) and the published data (Zhang *et al*., 2015), this compound was deduced as quercitrin. Other compounds were identified by a similar method. The detected accurate mass values of deprotonated molecular ion and fragment ions were compared with those published data in kinds of literature or/and the mass spectrometric data of reference standards shown in Fig. 5. In general, flavonol glycosides were the main flavonoids in EFA and the principal component was quercitrin.

Antioxidant Activity of EFA

As redundant ROS may damage skin cells and accelerate skin aging, the antioxidant effects of extracts isolated from plants should be ascertained to make sure whether the natural products are suitable for developing skin-care products. For this reason, the antioxidant activity of EFA was evaluated by the DPPH method, ABTS method, and reducing capacity.

The DPPH method is a typical antioxidant assay for evaluating the antioxidant activity of natural products in vitro. In the reaction, DPPH is applied as a free radical and used to evaluate the ability of antioxidants to bind to free radicals. It was found that EFA reduced DPPH in a dose-dependent fashion (Fig. 6A) and the DPPH scavenging potential of EFA (IC_{50}:90.91±3.36 μg/mL) was lower than that of V_C (IC_{50}: 43.08±0.60 μg/mL) (Table 4). In the case of the $ABTS^+$ scavenging assay, which is a combined electron transfer and hydrogen atom transfer assay, the $ABTS^+$ scavenging capacity of EFA was also in a dose-dependent manner (Fig. 6B). However, the $ABTS^+$ scavenging capacity of EFA (IC_{50}:15.09±0.17μg/mL) was higher than that of V_C (IC_{50}: 29.67±0.05μg/mL) (Table 4). The scavenging of $ABTS^+$ radical by EFA was relatively higher than DPPH radical scavenging activity. Similar to these results, You *et al*. (2011) also reported that the extracts of *Psidium guajava* exhibited potent ABTS radical scavenging activity which was higher than that of DPPH radical scavenging activity. This might be due to the stereoselectivity of the radicals or the solubility of the extract in different testing systems affecting the capacity of extracts to react and quench different radicals (Yu *et al*., 2002). Furthermore, the antioxidant activity of EFA was also evaluated by the reducing power assay. As shown in (Fig. 6C), the Fe^{3+} could be reduced to Fe^{2+} by EFA in a dose-dependent manner. The concentration for 50% of maximal effect (EC_{50}) of EFA was 67.69±2.97μg/mL which is slightly higher than that of Vc. All the above results indicated that EFA had good antioxidant activity.

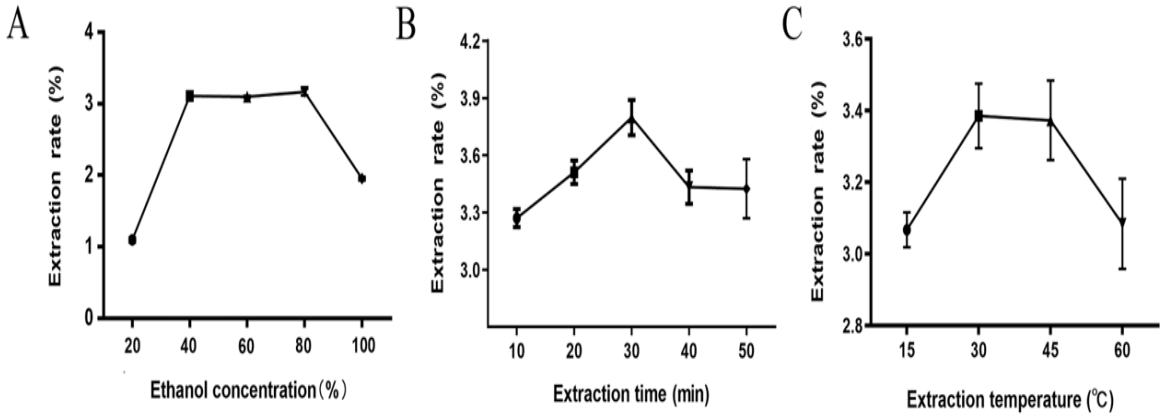

Fig. 2: The results of single-factor experiments. (A) ethanol concentrations (%); (B) extraction time (min); (C) extraction temperature (°C)

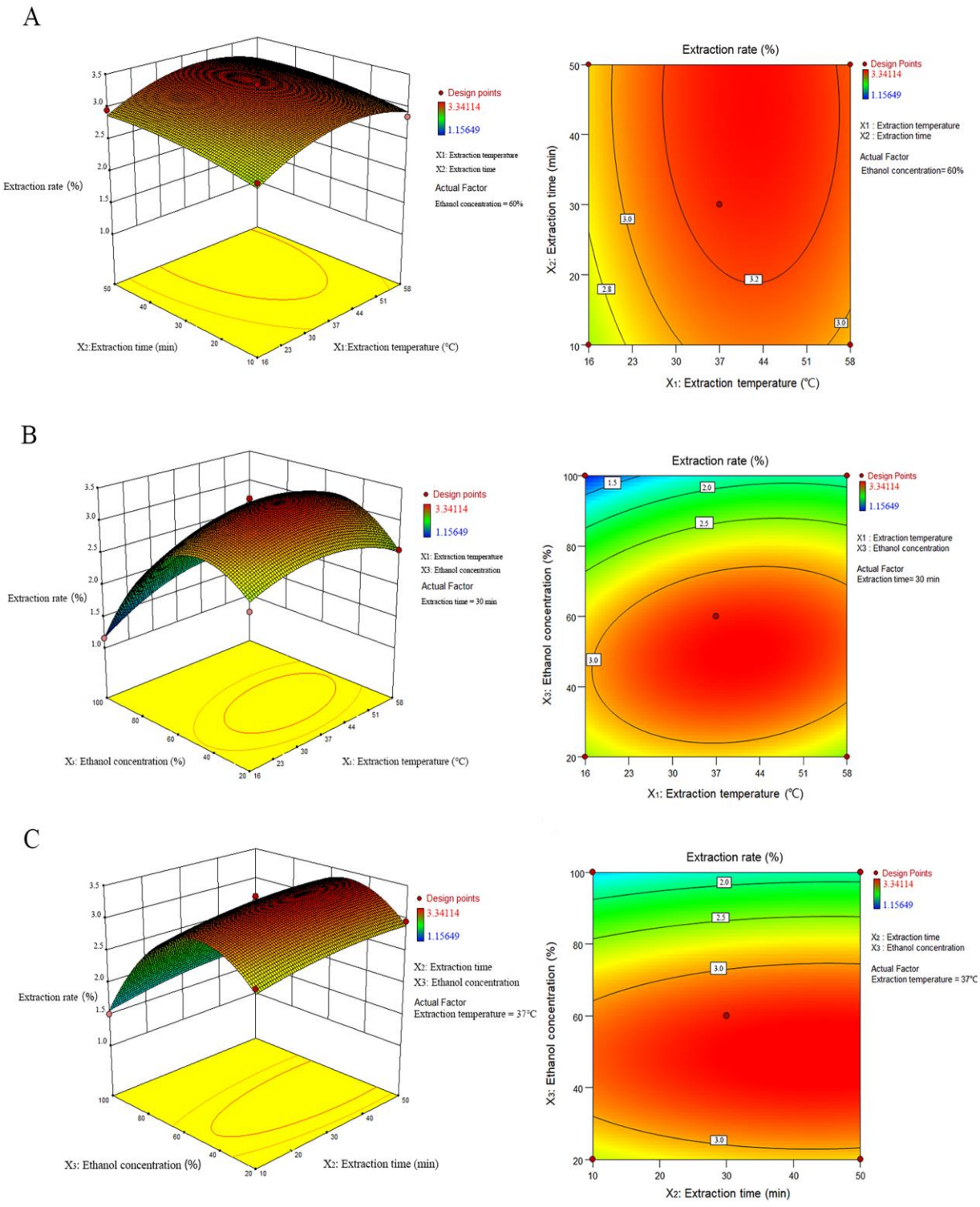

Fig. 3: The three-dimension response surface graphs and contour plots showing the correlative effects of extraction temperature, extraction time, and ethanol concentration on the extraction rate of total flavonoids. (A) extraction temperature versus extraction time; (B) extraction temperature versus ethanol concentration; (C) extraction time versus ethanol concentration

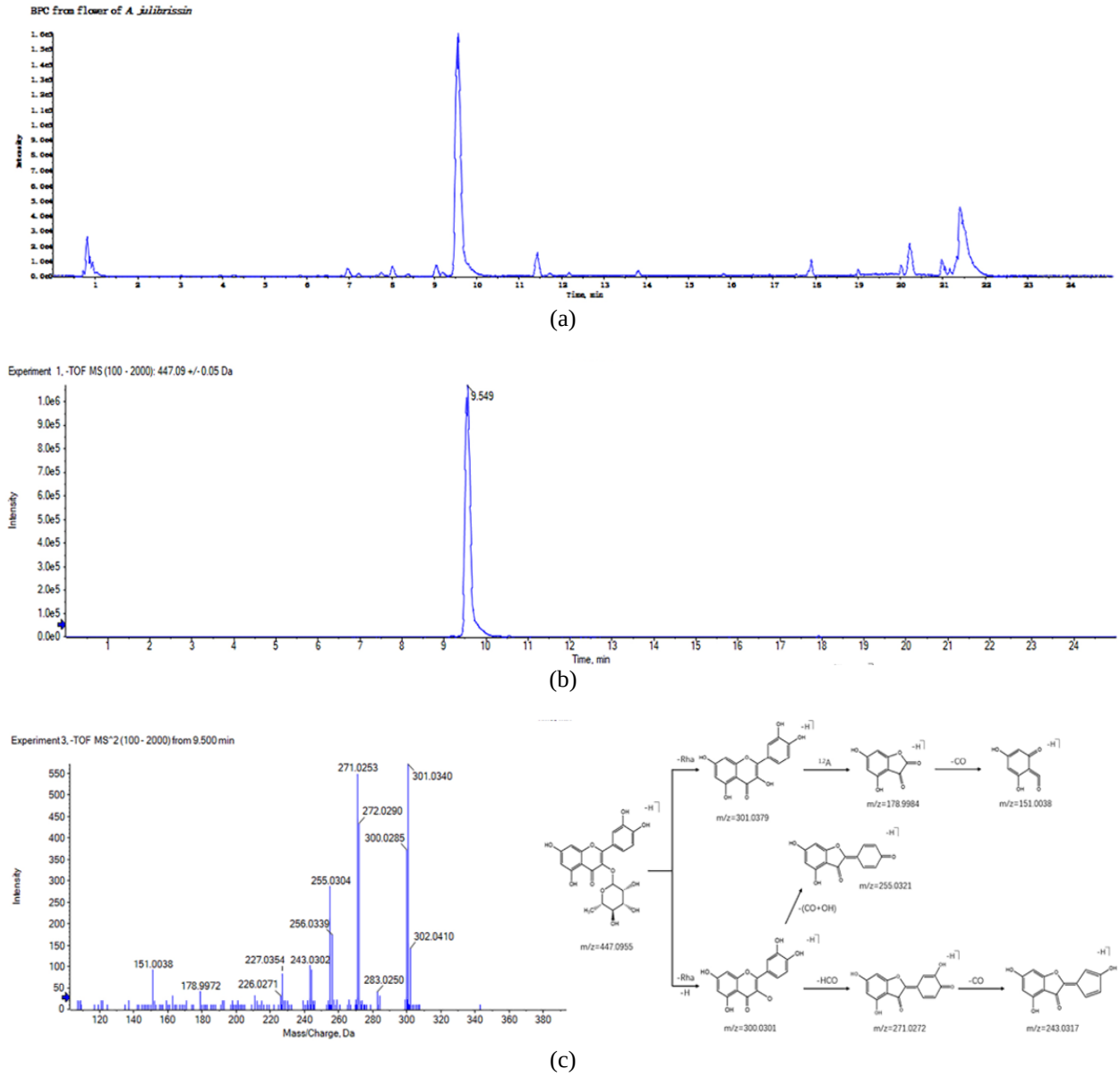

Fig. 4: Mass spectra of EFA and the fragmentation pattern of quercitrin. (A) Base peak chromatogram of EFA in a negative mode based on UPLC-QTOF-MS/MS; (B) Extracted ion chromatogram of quercitrin in EFA; (C) MS/MS spectra and postulated fragmentation pattern of quercitrin by means of ESI-QTOF in negative mode.

Tyrosinase Inhibitory Activity of EFA

Tyrosinase is the rate-limiting enzyme for the biosynthesis of melanin in the skin. It can catalyze the hydroxylation of monophenols to diphenols and further oxidize diphenols to o-quinone which is synthesized into melanin ultimately (Tian *et al*., 2019). The mushroom tyrosinase inhibitory essay is an effective method to screen melanogenesis inhibitors. Hence, the mushroom Tyrosinase Inhibitory Activity of EFA was tested to evaluate its anti-melanogenic activity. As shown in Fig. 7, the EFA suppressed tyrosinase activity in a dose-dependent manner, with an IC_{50} value of 1.32±0.01 mg/mL (Table 4). Although the IC_{50} value of EFA was higher than that of Vc, the EFA presented greater inhibitory activity against tyrosinase than those plant extracts previously reported owning good tyrosinase inhibitory activity (Sarikurkcu *et al*., 2020). From these results, it could be clearly stated that the EFA showed good tyrosinase inhibitory activity.

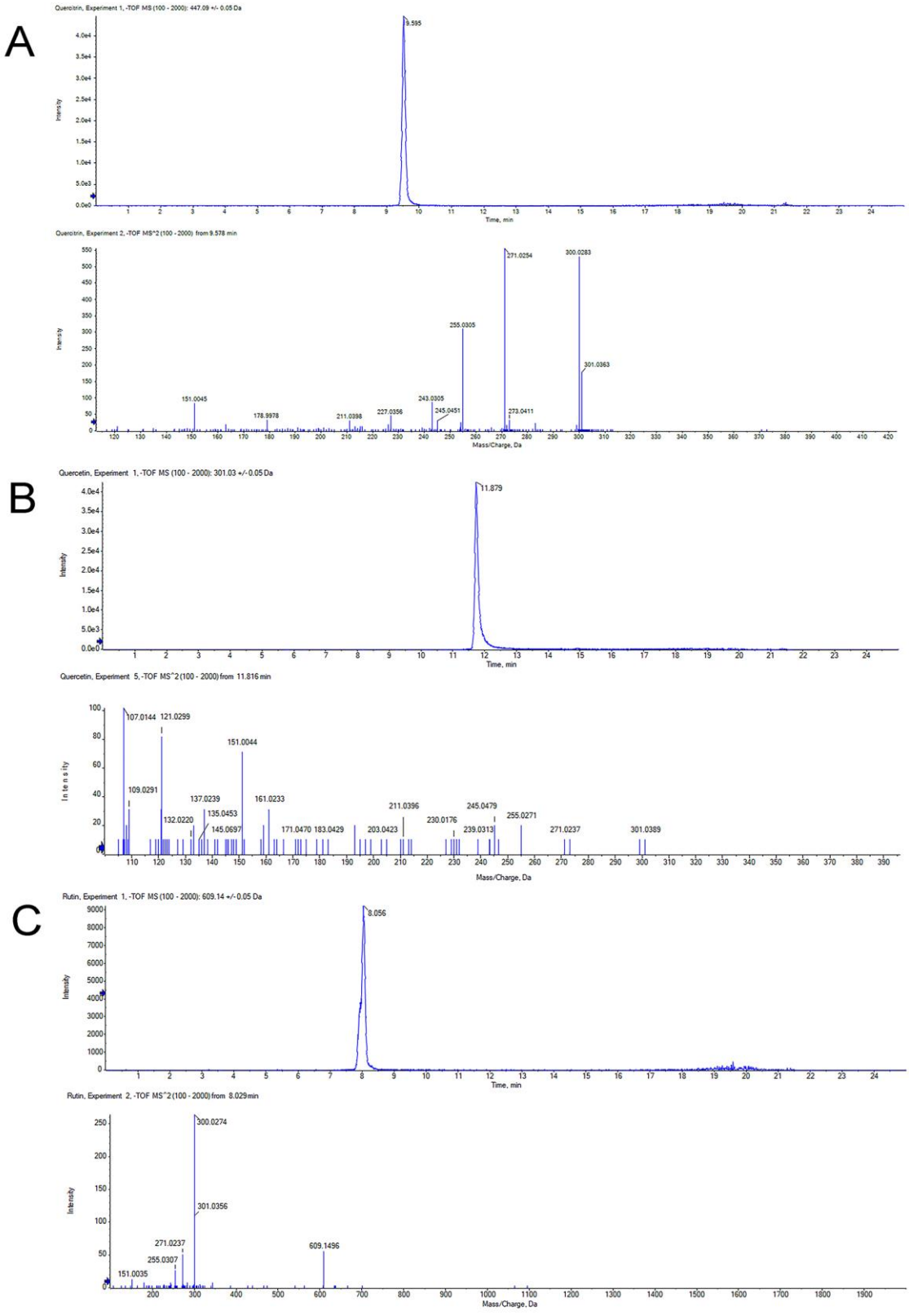

Fig. 5: The extracted ion chromatogram and MS/MS spectra of the reference standard by means of ESI-QTOF in negative mode. (A) quercitrin; (B) quercetin; (C) rutin

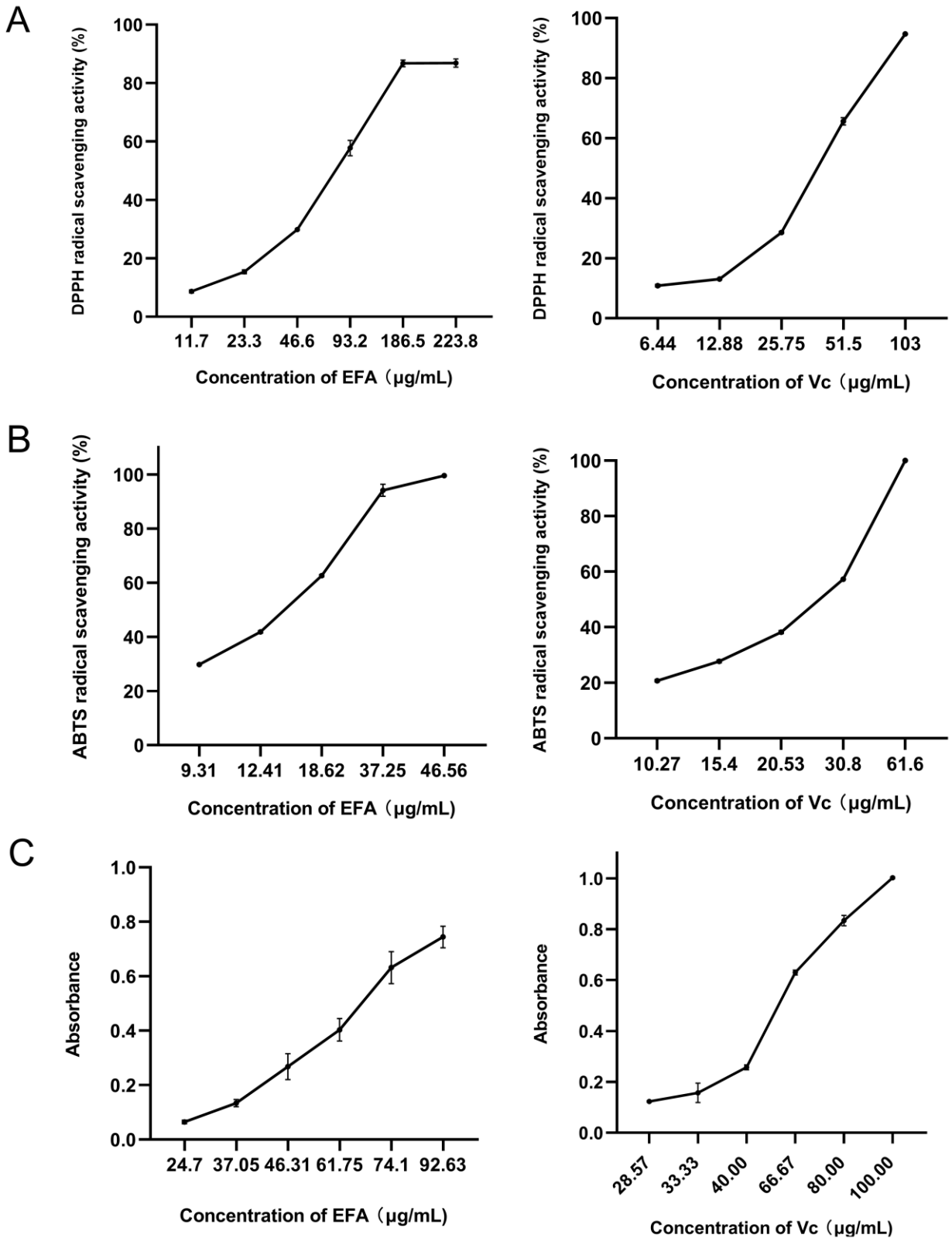

Fig. 6: Antioxidant activities of EFA and Vc. (A) the result of DPPH scavenging assay; (B) the result of ABTS scavenging assay; (C) the result of reducing power assay

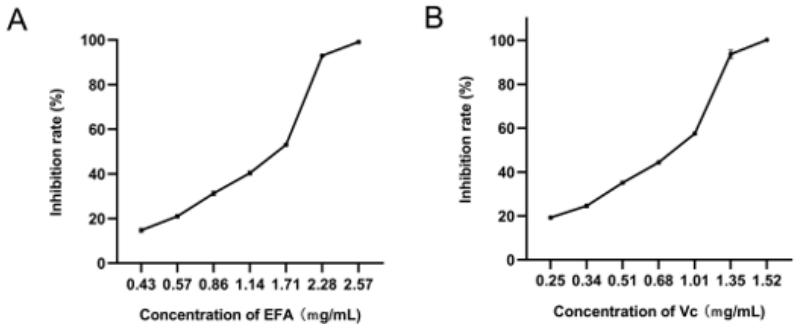

Fig. 7: The tyrosinase inhibitory activities of EFA and Vc. (A) the tyrosinase inhibitory activity of EFA; (B) the tyrosinase inhibitory activity of Vc

Table 2: ANOVA results of the RSM.

Source	Sum of squares	df	Mean square	F-value	P-value	Significant
Model	7.11	9.00	0.79	59.720	<0.0001	Significant
X_1	0.18	1.00	0.18	13.550	0.0078	*
X_2	0.12	1.00	0.12	8.910	0.0204	*
X_3	2.35	1.00	2.35	178.030	<0.0001	*
X_1X_2	5.30×10^{-4}	1.00	5.30×10^{-4}	0.040	0.8470	
X_1X_3	0.13	1.00	0.13	9.960	0.0160	*
X_2X_3	1.08×10^{-3}	1.00	1.08×10^{-3}	0.082	0.7830	
X_1^2	0.37	1.00	0.37	27.640	0.0012	*
X_2^2	0.029	1.00	0.029	2.210	0.1810	
X_3^2	3.72	1.00	3.72	281.700	<0.0001	*
Residual	0.093	7.00	0.013			
Lack of fit	0.076	3.00	0.025	6.050	0.0573	Not significant
Pure error	0.017	4.00	4.18×10^{-3}			
Corrected total	7.2	16.00				
R-Squared	0.9871					
Adj R-Squared	0.9706					
Pred R-Squared	0.8278					
Adeq Precision	23.911					

*Significant ($p < 0.05$)

Table 3: Flavonoids identified by UPLC-QTOF-MS/MS in EFA

Molecular No.	RT	[M-H]- Formula	[M-H]- Predicted	Error Measured	(-)-ESI-MS/MS (ppm)	Fragment Ions (m/z)	Identification
1	6.083	$C_{27}H_{30}O_{16}$	609.1461	609.1486	4.1	301.0418, 300.0296 271.0258, 255.0324, 243.0320	Isomer of rutin
2	6.174	$C_{33}H_{40}O_{20}$	755.204	755.208	5.3	755.2166, 301.0407, 300.0288 271.0247	Manghaslin (da Silva *et al*., 2021)[b]
3	6.417	$C_{27}H_{30}O_{16}$	609.1461	609.1496	5.7	301.0370, 300.0290 271.0268, 255.0311	Isomer of rutin
4	6.784	$C_{33}H_{40}O_{21}$	771.1989	771.0225	4.6	771.2137, 609.1534, 463.0931, 01.0360, 300.0295	Quercetin *3*-[glucosyl-(*1->3*)-rhamnosyl-(*1->6*)-galactoside] (El-Mousallamy, 1998)[b]
5	7.254	$C_{21}H_{20}O_{12}$	463.0882	463.0899	3.7	317.324, 316.0245, 287.0214 271.0264, 259.0263, 242.0229 214.0282, 151.0058	Myricetin-3-*O*-rhamnosid (Chaudhary *et al*., 2011)[b]
6	7.457	$C_{27}H_{30}O_{16}$	609.1461	609.1478	2.8	447.0992, 301.0385, 300.0289	Isomer of rutin
7	7.787	$C_{21}H_{20}O_{12}$	463.0882	463.0894	2.6	301.0366, 300.0291, 271.0263 255.0305, 243.0306, 151.0036	Hyperoside (Chaudhary *et al*., 2011)[b]
8	7.931	$C_{27}H_{30}O_{15}$	593.1512	593.1537	4.2	285.0412, 284.0323, 255.03, 227.0363	Kaempferol-3-*O*-rutinoside (Yang *et al*., 2021)
9	7.978	$C_{21}H_{20}O_{12}$	463.0882	463.0905	5	301.0371, 300.0288, 271.0254 255.03, 243.0301, 227.0368 179.0001, 151.0045	Isoquercitrin (Fernández-Agulló *et al*., 2020)
10	7.99	$C_{27}H_{30}O_{16}$	609.1461	609.1496	5.7	301.0383, 300.0277, 217.0235, 255.0315	Rutin (Ismail *et al*., 2019)[ab]
11	8.157	$C_{26}H_{28}O_{15}$	579.1355	579.1384	4.9	415.0661, 301.0389, 300.0290, 271.0258, 255.0313	Quercetin-3-*O*-xylopyranosyl (1→2)-rhamnopyranoside (Yang *et al*., 2021)
12	8.355	$C_{20}H_{18}O_{11}$	433.0776	433.0797	4.8	301.0395, 300.0302, 271.0262 255.0308, 243.0309, 151.0038	Avicularin (Chaudhary *et al*., 2011)[b]
13	8.504	$C_{27}H_{30}O_{16}$	609.1461	609.1488	4.4	447.0969, 301.0381 300.0274, 271.0290	Isomer of rutin
14	8.587	$C_{20}H_{18}O_{11}$	433.0776	433.0797	4.8	301.0350, 300.0283, 271.0258 255.0305, 243.0296, 151.0023	Reynoutrin (Chaudhary *et al*., 2011)[b]

Table 3: Continue

15	9.16	$C_{21}H_{20}O_{11}$	447.0933	447.0952	4.3	285.0425, 284.0337, 271.0147, 255.0312, 227.0344	Kaempferol-3-*O*-*β*-D-glucopyranoside (Yang *et al*., 2021)
16	9.556	$C_{21}H_{20}O_{11}$	447.0933	447.0955	5	301.0379, 300.0301, 271.0272 255.0321, 243.0317, 227.0363 178.9984, 151.0038	Quercitrin (Zhang *et al*., 2015)[a]
17	9.556	$C_{39}H_{50}O_{25}$	917.1841	917.1808	-3.6	917.1806, 447.0993, 301.0383 300.0303, 271.0251	Quercetin 3-rhamnosyl-(1->6)-[glucosyl-(1->2)-glucoside]-7-rhamnoside (National Center for Biotechnology Information, 2022) [b]
18	9.827	$C_{26}H_{28}O_{14}$	563.1406	563.1431	4.4	285.0355, 284.0355 255.0316, 227.0369	Kaempferol-3-*O*-xylopyranosyl (1→2)-rhamnopyranoside (Yang *et al*., 2021)
19	9.839	$C_{27}H_{30}O_{15}$	593.1512	593.155	6.4	285.0424, 284.0354 255.0332, 227.0333	Isomer of kaempferol-3-*O*-rutinoside
20	10.26	$C_{20}H_{18}O_{10}$	417.0827	417.0848	5	285.0435, 284.0337 255.0313, 227.0358	Kaempferol-3-*O*-α-D-arabinopyranoside (Yang *et al*., 2021)
21	10.92	$C_{20}H_{18}O_{10}$	417.0827	417.0838	2.6	285.0422, 284.0335, 225.0310 227.0372, 185.0656	Isomer of Kaempferol-3-*O*-α-D-arabinopyranoside
22	11.434	$C_{21}H_{20}O_{10}$	431.0984	431.1	3.8	285.0425, 284.0348, 255.0307 229.0516, 227.0353	Afzelin (Yang *et al*., 2021)
23	11.836	$C_{15}H_{10}O_7$	301.0354	301.0359	1.7	271.0237, 255.0175, 161.0233 151.0044, 121.0299, 107.0144	Quercetin (Yang *et al*., 2021)[a]
24	12.26	$C_{15}H_{12}O_5$	273.0758	273.076	0.9	153.0173	Naringenin (Yang *et al*., 2021)
25	15.462	$C_{31}H_{28}O_{14}$	623.1406	623.1454	7.7	623.1369, 447.0967, 301.0372 300.0289, 271.0260, 255.0280 243.0443, 151.0044	Isomer of 3″-O-(E)-feruloylquercitrin
26	15.504	$C_{30}H_{26}O_{13}$	593.1301	593.134	6.6	301.0357, 300.0295, 271.0256 255.03, 243.0293, 229.055	Isomer of 3″-(E)-p-Coumaroylquercitrin
27	15.685	$C_{30}H_{26}O_{13}$	593.1301	593.1329	4.8	301.0383, 300.0296, 271.0283 255.0305, 227.0334	3″-(*E*)-p-Coumaroylquercitrin (Yahagi *et al*., 2012)
28	15.805	$C_{31}H_{28}O_{14}$	623.1406	623.1451	7.2	447.0987, 301.0375, 300.0296 271.0256, 255.0319	3″-O-(*E*)-Feruloylquercitrin (Yahagi *et al*., 2012)
29	16.189	$C_{30}H_{26}O_{13}$	593.1301	593.1332	5.3	301.0360, 300.0292, 271.0263 255.0305, 229.0515, 151.0038	Isomer of 3″-(*E*)-p-Coumaroylquercitrin
30	16.452	$C_{31}H_{28}O_{14}$	623.1406	623.1447	6.5	301.0373, 300.0288, 271.0264 255.0299, 151.0044	Isomer of 3″-O-(*E*)-feruloylquercitrin
31	17.17	$C_{30}H_{26}O_{12}$	577.1352	577.1374	3.9	300.0279, 271.0245 255.0312, 174.9538	Isomer of 3″-(*E*)-Cinnamoylquercitrin
32	17.81	$C_{30}H_{26}O_{12}$	577.1352	577.1388	6.3	301.0327, 300.0279, 271.0255 255.0291, 243.033, 147.0442	3″-(*E*)-Cinnamoylquercitrin (Yahagi *et al*., 2012)

a: Identified by comparing with the reference standards
b: Compound identified in He Huan Hua for the first time

Table 4: Antioxidative and tyrosinase inhibitory activities of EFA and Vc.

Sample	DPPH (IC_{50}) (μg/mL)	$ABTS^+$(IC_{50}) (μg/mL)	Reducing power (EC_{50}) (μg/mL)	Tyrosinase inhibitory activity (IC_{50}) (mg/mL)
EFA	90.91 ± 3.36*	15.09 ± 0.17*	67.69 ± 2.97*	1.32 ± 0.01*
Vc	43.08 ± 0.60	29.67 ± 0.05	58.09 ± 0.82	0.74 ± 0.02

*Significant ($p<0.05$)

Discussion

For characterization of chemical profile and assessment of biological activities, the extraction method should be optimized for adequate extraction of target ingredients. In this study, the actual yield rate of total flavonoids from 'He Huan Hua' obtained by ultrasonic-assisted extraction is up to 3.31%, which is higher than that previously reported by cold soak (yield rate of total flavonoids was 2.53%) (Yuan *et al*., 2012). Xie *et al*. (2017) also found that ultrasonic-assisted extraction was more effective and convenient than other conventional extraction methods when used to extract flavonoids from plants. It is indicated that ultrasonic-assisted extraction is fit for total flavonoid extraction from 'He Huan Hua'.

In single-factor experiments, the extraction yield of total flavonoids increased first and then decreased with continuous incensement of ethanol concentration, extraction temperature, and extraction time, which might be attributed to the change of extraction solvent polarity and stability of flavonoids (Yuan *et al*., 2015). Afterward, RSM was used to predict optimum experimental factors. Based on the graphical analysis of response surfaces and the results of ANOVA, it indicated that these three factors had different effects on the extraction rate of total flavonoids in EFA. The sequence was as follows: Ethanol concentration > extraction temperature > extraction time. Song *et al*. (2014) previously showed that the extraction yield of quercitrin from 'He Huan Hua' was dependent on ethanol concentration and extraction temperature when performed by ultrasonic-assisted extraction method and the influence of ethanol concentration was most significant. It was similar to the present results. After illustrating the influence of the three extraction factors, the optimized process parameters were obtained according to the RSM regression equation. The actual extraction rate of total flavonoids by the predicted methods was similar to the predicted value with a deviation of less than 3%. In summary, this condition suggests that the established response surface model could be effectively used to optimize the parameters for ultrasonic-assisted

extraction of flavonoids from ‘He Huan Hua’.

To characterize the chemical profile of ‘He Huan Hua’, UHPLC-QTOF-MS/MS which own high efficiency and excellent accuracy was used (Aabideen *et al*., 2021, Aloo *et al*., 2021). In this research, a total of 32 different flavonoids were identified and the main components in EFA were flavonol glycosides, such as quercitrin, rutin, and kaempferol-3-O-glucopyranoside. These flavonol compounds contain more hydroxyl groups. As hydrogen from the hydroxyl groups of flavonoids could scavenge active oxygen free radicals, the flavonoid with more hydroxyl group exhibited better antioxidant activity (Islam *et al*., 2020; Ekaette and Saldaña, 2021; Shen *et al*., 2021). It had been reported that quercetin, kaempferol, and their glycoside derivatives could reduce the damage of ROS in vivo and scavenge free radicals in vitro exhibiting higher antioxidant capacity (Fuentes *et al*., 2021; de Lima Júnior *et al*., 2021). The results of this research also indicated that EFA owns good antioxidant activity. Therefore, it can be concluded that the good antioxidant activity of EFA may have a close relationship with the presence of flavonols in ‘He Huan Hua’.

Flavonol is an important natural product that is widely distributed in plants. Previous studies have verified the importance of flavonol to control hyperpigmentation via the inhibition of the tyrosinase enzyme (Lin *et al*., 2008). The chemical profile of EFA showed that ‘He Huan Hua’ was rich in flavonol glycosides and the extracts had good tyrosinase inhibitory activity. It is speculated that the flavonol compounds in EFA may be contributed to its tyrosinase inhibitory activity. The molecular docking analysis demonstrated that the hydroxyl substitutions at C-7, C-3', and C-4' in the structure of flavonol had crucial value for competitive inhibition of tyrosinase (Şöhretoğlu *et al*., 2018). The presence of 3-O-rhamnosylmoiety in flavonol was also suggested to participate in tyrosinase inhibition (El-Nashar *et al*., 2021). As shown in Table 3, most flavonols identified in EFA owned hydroxyl substitution at C-7, C-3', and/or C-4’. Quercitrin, the principal component in EFA, has a 3-O-rhamnosylmoiety (Fig. 4). Previous studies have proved that kaempferol-3-O-rutinoside, rutin, and quercetin possessed potent inhibitory activity on tyrosinase compared to the standard drug, kojic acid (Santi *et al*., 2019, Zhou *et al*., 2019). These three flavonols were also rich in EFA (shown in Table 3 and Fig. 4). Hence, it can be concluded that the tyrosinase inhibitory of EFA may be due to the rich presence of flavonols, and 'He Huan Hua' has potent value for developing effective tyrosinase inhibitors. However, the effective and specific compounds in EFA for tyrosinase inhibitors have not been screened and clarified. It is worth to be a further investigation in future studies.

Conclusion

The multi-response optimization of ultrasonic-assisted total flavonoid extraction from ‘He Huan Hua’ was successfully processed by RSM. The optimal extraction parameters were as follows: Ethanol concentration of 49%, extraction time of 43 min, and extraction temperature of 40°C. There was no significant difference between the actual extraction rate under optimized conditions and the result predicted by the model. The extraction yield of total flavonoids from 'He Huan Hua' under the optimized method was higher than that of other conventional methods. The chemical profile of EFA was identified with a total of 32 compounds which were mainly flavonols. The EFA also showed good antioxidant and tyrosinase inhibitory activities, probably due to the high content of flavonols. In summary, the present study not only established an effective and convenient method for total flavonoid extraction from 'He Huan Hua' but also definitively characterized the chemical profile of ’He Huan Hua’. More importantly, it also revealed the antioxidant and tyrosinase inhibitory activities of extracts of ‘He Huan Hua’. The flavonoids in ‘He Huan Hua’ had great application values in the development of effective antioxidants and tyrosinase inhibitors for the prevention of premature skin aging.

Nomenclature and Abbreviation Section

‘He Huan Hua’:	The flower of *Albizia julibrissin*
Flavonol:	A class of flavonoid compounds
EFA:	Extracts of the flower of *Albizia julibrissin*
HPLC-QTOF-MS/MS:	High-Performance Liquid Chromatography coupled with Quadrupole Time-of-Flight Tandem Mass Spectrometry. An instrument widely used for characterization of chemical profile
RSM:	Response Surface Methodology
ROS:	Reactive oxygen species
DPPH:	Diphenyl Picryl Hydrazinyl radical
ABTS:	2,2′-Azinobis (3-Ethylbenzothiazoline-6-sulfonic acid)
IC_{50}:	The half-maximal Inhibitory Concentration
EC_{50}:	Concentration for 50% of maximal effect

Acknowledgment

We thank professor Minjian Qin at China Pharmaceutical University for plant identification.

Funding Information

This study was supported by the National Natural Science Foundation of China [Grant number 82003885], the Foreign academician workstation of Suzhou city [Grant number SWY2020001], and Jiangsu Pharmaceutical Association-TianQing hospital pharmacy research [Grant number Q202127].

Author's Contributions

Yijie Cheng and Yuwen Zhang: Optimized the extraction method and wrote the study.

Hanzhang Sun and Dongting Huang: Performed the antioxidant assessment and tyrosinase inhibitory assay.

Bo Jiang: Characterized the chemical profile of EFA.

Jingyuan Xu: Conceived the project, designed the experiments and revised and polished the manuscript.

Ethics

This article is original and contains unpublished material. The corresponding author confirms that all of the other authors have read and approved the manuscript and that no ethical issues are involved.

References

Aabideen, Z. U., Mumtaz, M. W., Akhtar, M. T., Raza, M. A., Mukhtar, H., Irfan, A., & Saari, N. (2021). Cassia fistula Leaves; UHPLC-QTOF-MS/MS-based metabolite profiling and molecular docking insights to explore bioactive role towards inhibition of pancreatic lipase. Plants, 10(7), 1334. doi.org/ 10.3390/plants10071334

Ahmad, A., Alkharfy, K. M., Wani, T. A., & Raish, M. (2015). Application of Box–Behnken design for ultrasonic-assisted extraction of polysaccharides from Paeonia emodi. International journal of biological macromolecules, 72, 990-997. doi.org/10.1016/j.ijbiomac.2014.10.011

Aloo, S. O., Ofosu, F. K., Daliri, E. B. M., & Oh, D. H. (2021). UHPLC-ESI-QTOF-MS/MS Metabolite Profiling of the Antioxidant and Antidiabetic Activities of Red Cabbage and Broccoli Seeds and Sprouts. Antioxidants, 10(6), 852. doi.org/10.3390/antiox10060852

Arroo, R. R., Sari, S., Barut, B., Özel, A., Ruparelia, K. C., & Şöhretoğlu, D. (2020). Flavones as tyrosinase inhibitors: Kinetic studies in vitro and in silico. Phytochemical Analysis, 31(3), 314-321. doi.org/10.1002/pca.2897

Bourhim, T., Villareal, M. O., Couderc, F., Hafidi, A., Isoda, H., & Gadhi, C. (2021). Melanogenesis promoting effect, antioxidant activity, and UPLC-ESI-HRMS characterization of phenolic compounds of argan leave extract. Molecules, 26(2), 371. doi.org/ 10.3390/molecules26020371

Chaudhary, A., Kaur, P., Kumar, N., Singh, B., Awasthi, S., & Lal, B. (2011). Chemical fingerprint analysis of phenolics of Albizia Chinensis based on ultra-performance LC-electrospray ionization-quadrupole time-of-flight mass spectrometry and antioxidant activity. Natural Product Communications, 6(11), 1934578X1100601115. doi.org/10.1177/1934578x1100601115

CPC. (2020). Pharmacopoeia of the People's Republic of China; Chinese Medical Science and Technology Press: Beijing, China, 1, pp, 150.

Cruciani, S., Trenta, M., Rassu, G., Garroni, G., Petretto, G. L., Ventura, C., & Pintore, G. (2021). Identifying a role of red and white wine extracts in counteracting skin aging: Effects of antioxidants on fibroblast behavior. Antioxidants, 10(2), 227. doi.org/10.3390/antiox10020227

Cui, H., Pan, H. W., Wang, P. H., Yang, X. D., Zhai, W. C., Dong, Y., & Zhou, H. L. (2018). Essential oils from carex meyeriana Kunth: Optimization of hydrodistillation extraction by response surface methodology and evaluation of its antioxidant and antimicrobial activities. Industrial Crops and Products, 124, 669-676. doi.org/10.1016/j.indcrop.2018.08.041

da Silva, R. G., Almeida, T. C., Reis, A. C. C., Filho, S. A. V., Brandão, G. C., da Silva, G. N., & de Souza, G. H. B. (2021). In silico pharmacological prediction and cytotoxicity of flavonoid glycosides identified by UPLC-DAD-ESI-MS/MS in extracts of Humulus lupulus leaves cultivated in Brazil. Natural Product Research, 35(24), 5918-5923. doi.org/10.1080/14786419.2020.1803308

de Lima Júnior, J. P., Franco, R. R., Saraiva, A. L., Moraes, I. B., & Espindola, F. S. (2021). Anacardium humile St. Hil is a novel source of antioxidant, antiglycation, and α-amylase inhibitor molecules with potential for the management of oxidative stress and diabetes. Journal of Ethnopharmacology, 268, 113667. doi.org/10.1016/j.jep.2020.113667

Ekaette, I., & Saldaña, M. D. (2021). Ultrasound processing of rutin in food-grade solvents: Derivative compounds, antioxidant activities, and optical rotation. Food Chemistry, 344, 128629. doi.org/10.1016/j.foodchem.2020.128629

El-Mousallamy, A. M. (1998). Leaf flavonoids of Albizia lebbeck. Phytochemistry, 48(4), 759-761. doi.org/10.1016/s0031-9422(97)01117-5

El-Nashar, H. A., El-Din, M. I. G., Hritcu, L., & Eldahshan, O. A. (2021). Insights on the Inhibitory Power of Flavonoids on Tyrosinase Activity: A Survey from 2016 to 2021. Molecules, 26(24), 7546. doi.org/10.3390/molecules26247546

Fernández-Agulló, A., Castro-Iglesias, A., Freire, M. S., & González-Álvarez, J. (2020). Optimization of the extraction of bioactive compounds from walnut (Juglans major 209 x Juglans regia) leaves Antioxidant capacity and phenolic profile. Antioxidants, 9(1), 18. doi.org/10.3390/antiox9010018

Fuentes, J., de Camargo, A. C., Atala, E., Gotteland, M., Olea-Azar, C., & Speisky, H. (2021). Quercetin oxidation metabolite present in Onion peel protects Caco-2 cells against oxidative stress, NF-kB activation, and loss of epithelial barrier function induced by NSAIDs. Journal of Agricultural and Food Chemistry, 69(7), 2157-2167. doi.org/10.1021/acs.jafc.0c07085

Ha, T. J., Park, J. E., Lee, K. S., Seo, W. D., Song, S. B., Lee, M. H., & Lee, J. H. (2021). Identification of anthocyanin compositions in black seed coated Korean adzuki bean (*Vigna angularis*) by NMR and UPLC-Q-Orbitrap-MS/MS and screening for their antioxidant properties using different solvents systems. Food Chemistry, 346, 128882. doi.org/10.1016/j.foodchem.2020.128882

Hałdys, K., Goldeman, W., Jewgiński, M., Wolińska, E., Anger, N., Rossowska, J., & Latajka, R. (2018). Inhibitory properties of aromatic thiosemicarbazones on mushroom tyrosinase: Synthesis, kinetic studies, molecular docking, and effectiveness in melanogenesis inhibition. Bioorganic chemistry, 81, 577-586. doi.org/10.1016/j.bioorg.2018.09.003

Islam, S., Alam, M. B., Ahmed, A., Lee, S., Lee, S. H., & Kim, S. (2020). Identification of secondary metabolites in Averrhoa carambola L. bark by high-resolution mass spectrometry and evaluation for α-glucosidase, tyrosinase, elastase, and antioxidant potential. Food Chemistry, 332, 127377. doi.org/10.1016/j.foodchem.2020.127377

Ismail, B. B., Pu, Y., Guo, M., Ma, X., & Liu, D. (2019). LC-MS/QTOF identification of phytochemicals and the effects of solvents on phenolic constituents and antioxidant activity of baobab (*Adansonia digitata*) fruit pulp. Food Chemistry, 277, 279-288. doi.org/10.1016/j.foodchem.2018.10.056

Kang, T. H., Jeong, S. J., Kim, N. Y., Higuchi, R., & Kim, Y. C. (2000). The sedative activity of two flavonol glycosides isolated from the flowers of Albizzia julibrissin Durazz. Journal of ethnopharmacology, 71(1-2), 321-323. doi.org/10.1016/s0378-8741(99)00202-0

Khochapong, W., Ketnawa, S., Ogawa, Y., & Punbusayakul, N. (2021). Effect of in vitro digestion on bioactive compounds, antioxidant and antimicrobial activities of coffee (*Coffea arabica L.*) pulp aqueous extract. Food Chemistry, 348, 129094. doi.org/10.1016/j.foodchem.2021.129094

Lavigne, E. G., Cavagnino, A., Steinschneider, R., Breton, L., Baraibar, M. A., & Jäger, S. (2022). Oxidative damage prevention in human skin and sensory neurons by a salicylic acid derivative. Free Radical Biology and Medicine. doi.org/10.1016/j.freeradbiomed.2022.01.029

Lee, J., Kim, H. J., Lee, S. J., & Lee, M. S. (2021). Effects of Hahella chejuensis-derived prodigiosin on UV-induced ROS production, inflammation, and cytotoxicity in HaCaT human skin keratinocytes. doi.org/10.4014/jmb.2011.11024

Li, M. X., Xie, J., Bai, X., & Du, Z. Z. (2021). Anti-aging potential, anti-tyrosinase, and antibacterial activities of extracts and compounds isolated from Rosa chinensis cv. 'Jin Bian'. Industrial Crops and Products, 159, 113059. doi.org/10.1016/j.indcrop.2020.113059

Lin, J. W., Chiang, H. M., Lin, Y. C., & Wen, K. C. (2008). Natural products with skin-whitening effects. Journal of Food and Drug Analysis, 16(2). doi.org/10.38212/2224-6614.2366

NCBI. (2022). PubChem Compound Summary for CID 44259297. National Center for Biotechnology Information https://pubchem.ncbi.nlm.nih.gov/compound/44259297.

Sady, S., Matuszak, L., & Błaszczyk, A. (2019). Optimization of ultrasonic-assisted extraction of bioactive compounds from chokeberry pomace using response surface methodology. Acta Scientiarum Polonorum Technologia Alimentaria, 18(3), 249-256. doi.org/10.17306/J.AFS.2019.0673

Santi, M. D., Bouzidi, C., Gorod, N. S., Puiatti, M., Michel, S., Grougnet, R., & Ortega, M. G. (2019). In vitro biological evaluation and molecular docking studies of natural and semisynthetic flavones from Gardenia oudiepe (Rubiaceae) as tyrosinase inhibitors. Bioorganic chemistry, 82, 241-245. doi.org/10.1016/j.bioorg.2018.10.034

Sarikurkcu, C. andrade, J. C., Ozer, M. S., de Lima Silva, J. M. F., Ceylan, O., de Sousa, E. O., & Coutinho, H. D. M. (2020). LC-MS/MS profiles and interrelationships between the enzyme inhibition activity, total phenolic content, and antioxidant potential of Micromeria Nervosa extracts. Food Chemistry, 328, 126930. doi.org/10.1016/j.foodchem.2020.126930

Sarikurkcu, C., Tepe, B., Kocak, M. S., & Uren, M. C. (2015). Metal concentration and antioxidant activity of edible mushrooms from Turkey. Food Chemistry, 175, 549-555. doi.org/10.1016/j.foodchem.2014.12.019

Shen, J., Hu, M., Tan, W., Ding, J., Jiang, B., Xu, L., ... & Xiao, P. (2021). Traditional uses, phytochemistry, pharmacology, and toxicology of Coreopsis tinctoria Nutt.: A review. Journal of Ethnopharmacology, 269, 113690. doi.org/10.1016/j.jep.2020.113690

Şöhretoğlu, D., Sari, S., Barut, B., & Özel, A. (2018). Tyrosinase inhibition by some flavonoids: Inhibitory activity, the mechanism by in vitro and in silico studies. Bioorganic chemistry, 81, 168-174. doi.org/10.1016/j.bioorg.2018.08.020

Song, L. D., Z. X. Wang, Q. Zhang, N. Zhang & B. W. Jiang. (2014). Optimization of ultrasound-assisted extraction quercitrin from *Albizia Julibrissin* via response surface methodology. Strait Pharmaceutical Journal, 26-01, 22-24. doi.org/10.3969/j.issn.1006-3765.2014.01.006

Sunday, N. F. (2020). Chemometrics of solvent extraction of Mn (II) and Fe (III) bis (salicylidene) ethylenediamine complexes in acid medium. Journal of Human, Earth, and Future, 1(2), 71-77. DOI. org/ 10.28991/HEF-2020-01-02-03

Tian, J. L., Liu, T. L., Xue, J. J., Hong, W., Zhang, Y., Zhang, D. X., & Niu, S. L. (2019). Flavanoids derivatives from the root bark of Broussonetia papyrifera as a tyrosinase inhibitor. Industrial Crops and Products, 138, 111445. doi.org/10.1016/j.indcrop.2019.06.008

Xie, G., Li, R., Han, Y., Zhu, Y., Wu, G., & Qin, M. (2017). Optimization of the extraction conditions for buddleja Officinalis maxim. using response surface methodology and exploration of the optimum harvest time. Molecules, 22(11), 1877. doi.org/10.3390/molecules22111877

Xie, H., Huang, J., Woo, M. W., Hu, J., Xiong, H., & Zhao, Q. (2021). Effect of cold and hot enzyme deactivation on the structural and functional properties of rice dreg protein hydrolysates. Food Chemistry, 345, 128784. doi.org/10.1016/j.foodchem.2020.128784

Yahagi, T., Daikonya, A., & Kitanaka, S. (2012). Flavonol acylglycosides from the flower of *Albizia julibrissin* and their inhibitory effects on lipid accumulation in 3T3-L1 cells. Chemical and Pharmaceutical Bulletin, 60(1), 129-136. doi.org/10.1248/cpb.60.129

Yang, D., Wang, L., Zhai, J., Han, N., Liu, Z., Li, S., & Yin, J. (2021). Characterization of antioxidant, α-glucosidase, and tyrosinase inhibitors from the rhizomes of Potentilla anserina L. and their structure-activity relationship. Food Chemistry, 336, 127714. doi.org/10.1016/j.foodchem.2020.127714

Yang, Y., Sun, X., Ni, H., Du, X., Chen, F., Jiang, Z., & Li, Q. (2019). Identification and characterization of the tyrosinase inhibitory activity of caffeine from camellia pollen. Journal of Agricultural and Food Chemistry, 67(46), 12741-12751. doi.org/10.1021/acs.jafc.9b04929

You, D. H., Park, J. W., Yuk, H. G., & Lee, S. C. (2011). Antioxidant and tyrosinase inhibitory activities of different parts of guava (Psidium guajava L.). Food Science and Biotechnology, 20(4), 1095-1100. doi.org/10.1007/s10068-011-0148-9

Yu, L., Haley, S., Perret, J., Harris, M., Wilson, J., & Qian, M. (2002). Free radical scavenging properties of wheat extracts. Journal of agricultural and food chemistry, 50(6), 1619-1624. doi.org/org/10.1021/jf010964p

Yu, Z. X., Zhang, Y. Y., Zhao, X. X., Yu, L., Chen, X. B., Wan, H. T., & Jin, W. F. (2021). Simultaneous optimization of ultrasonic-assisted extraction of Danshen for maximal tanshinone IIA and salvianolic acid B yields and antioxidant activity: A comparative study of the response surface methodology and artificial neural network. Industrial Crops and Products, 161, 113199. 113199. doi.org/10.1016/j.indcrop.2020.113199

Yuan J. M., W. Y. Guo & Y. L. Wang. (2012). Study on extraction technology and hydroxyl free radical scavenging ability of total flavonoids from the flower of *silk tree albizzia.* China Food Additives, (01), 87-91. doi.org/10.3969/j.issn.1006-2513.2012.01.008

Yuan, J. M., Lv, X. X., & Wang, C. F. (2013). Study on Extraction technology of polysaccharides from flos Albiziae and its antioxidition activity. Hubei Agricultural Sciences, 52-11, 2625-2628. doi.org/10.3969/j.issn.0439-8114.2013.11.044

Yuan, J., J. Huang, G. Wu, J.H. Tong, G.Y. Xie, J.A. Duan & M.J. Qin. (2015). Multiple responses optimization of ultrasonic-assisted extraction by Response Surface Methodology (RSM) for rapid analysis of bioactive compounds in the flower head of Chrysanthemum morifolium Ramat. Industrial Crops and Products, 74, 192-199. doi.org/10.1016/j.indcrop.2015.04.057

Zhang, Z., L. He, L. Lu, Y. Liu, G. Dong, J. M., & P. Luo. (2015). Characterization and quantification of the chemical compositions of Scutellariae Barbatae herba and differentiation from its substitute by combining UHPLC-PDA-QTOF-MS/MS with UHPLC-MS/MS. Journal of Pharmaceutical and Biomedical Analysis, 109, 62-66. doi.org/10.1016/j.jpba.2015.02.025

Zhou, Z., J. Hou, J. Xiong & M. Li. (2019). Characterization of sulfuretin as a depigmenting agent. Fundamental and clinical pharmacology, 33(2), 208–215. doi.org/10.1111/fcp.12414

Zuo, J., Ma, P., Geng, S., Kong, Y., Li, X., Fan, Z., Zhang, Y., Dong, A., & Zhou, Q. (2022). Optimization of the extraction process of flavonoids from *Trollius ledebouri* with natural deep eutectic solvents. Journal of separation science, 45-3, 717–727. doi.org/10.1002/jssc.202100802